

The Globular Cluster M15. I. Identification, Discovery, and Period Determination of Variable Stars

T. Michael Corwin

Department of Physics and Optical Science, University of North Carolina at Charlotte,
Charlotte, NC 28223

`mcorwin@uncc.edu`

J. Borissova

Departamento de Física y Astronomía, Facultad de Ciencias, Universidad de Valparaíso,
Casilla 5030, Valparaíso, Chile

`jura.borissova@uv.cl`

Peter B. Stetson

Dominion Astrophysical Observatory, Herzberg Institute of Astrophysics, National
Research Council of Canada, 5071 West Saanich Road, Victoria, BC V9E 2E7, Canada

`peter.stetson@nrc-cnrc.gc.ca`

M. Catelan

Pontificia Universidad Católica de Chile, Departamento de Astronomía y Astrofísica,
Av. Vicuña Mackenna 4860, 782-0436 Macul, Santiago, Chile

`mcatelan@astro.puc.cl`

Horace A. Smith

Dept. of Physics and Astronomy, Michigan State University, East Lansing, MI 48824

`smith@pa.msu.edu`

R. Kurtev

Departamento de Física y Meteorología, Facultad de Ciencias, Universidad de Valparaíso,
Casilla 5030, Valparaíso, Chile

`rkurtev@uv.cl`

and

Andrew W. Stephens

Gemini Observatory, 670 N. A'ohoku Place, Hilo, HI 96720

`stephens@gemini.edu`

Received _____; accepted _____

AJ, in preparation (March 28, 2008)

ABSTRACT

We present new *BVI* CCD photometry for variables in the globular cluster M15. Our photometry was obtained using both the image subtraction package ISIS and DAOPHOT/ALLFRAME. The data were acquired in 2001 on two observing runs on 11 observing nights using the 2-m telescope of the Bulgarian National Astronomical Observatory “Rozhen” with a Photometrics CCD camera. For 40 previously known variables, we present a period for the first time, and improved periods were obtained for many previously known variables. Fourteen new variables are reported. We present updated Bailey diagrams for the cluster and discuss its Oosterhoff classification. Although many of M15’s RRab pulsators fall at an intermediate locus between Oosterhoff types I and II in the Bailey diagram, we argue that M15 is indeed a bona-fide Oosterhoff type II globular cluster.

Subject headings: globular cluster: individual (M15) — stars: evolution — stars: variables: other

1. Introduction

The metal-poor globular cluster M15 = NGC 7078 ($[\text{Fe}/\text{H}] = -2.26$; Harris 1996) was one of the three original “type II” (OoII) clusters identified in Oosterhoff’s (1939) seminal paper. It is a post-core-collapse cluster with an extraordinarily dense center (Sosin & King 1997). Observations of its RR Lyrae variables have long been seen as important to clarifying the origin and nature of the Oosterhoff phenomenon. M15 is known to contain over 180 intrinsic variables, predominately RR Lyraes (Clement et al. 2001 and references therein).

RR Lyrae variables provide crucial information for estimating globular cluster ages and distances, as summarized by Smith (1995). They are easily identified by their distinctive light curves and are bright enough to be observed to considerable distances. Their absolute magnitudes appear to be quite restricted. The range of RR Lyrae luminosities is discussed, among others, in Carney (2001), Harris (2001), and Catelan (2007). Stellar variability studies of globular clusters are also of fundamental importance to understanding both stellar and cluster evolution, as well as to constrain the formation history of the Galaxy and its nearby satellites (Catelan 2007).

The variables in M15 were previously studied by Sandage, Katem, & Sandage (1981), Bingham et al. (1984), Silbermann & Smith (1995), Butler et al. (1998), Ó Tuairisg et al. (2003, hereafter OT03), Zheleznyak & Kravtsov (2003, hereafter ZK03), and Arellano Ferro, García Lugo, & Rosenzweig (2006) among others. In the present paper, we present the results of a new variability analysis of the cluster, carried out using both image-subtraction techniques and the standard DAOPHOT/ALLFRAME analysis. We provide periods for 39 previously known variables whose periods were unknown, improved periods for 30 previously known variables, and periods for 14 new variables. In §2, we discuss our observational material and reduction procedures. In §3, we present our periods and derived light curves in either absolute B magnitudes or relative B fluxes. §4 discusses standard magnitudes and

light curve amplitudes, as well as the cluster’s Oosterhoff classification, while §5 contains notes on individual stars. We close in §6 by summarizing our main results.

2. Observations and Data Reduction

2.1. Observations

Time-series photometry was obtained during the interval 2001 July 13 to 2001 July 19 with the 2-m Ritchey-Chrétien telescope of the Bulgarian National Astronomical Observatory “Rozhen” with a Photometrics CCD camera. This represents almost all of our data. During the interval 2001 September 18 to 2001 September 25, using the same telescope and instrument, a few additional images were obtained. The scale at the Cassegrain-focus CCD was 0.33 arcsec per pixel and the observing area was centered on the cluster center. In total 230 *B*, 201 *V*, and 163 *I* frames were obtained, with seeing between 0.8 and 1.2 arcsec. In order to resolve better the cluster center, we observed M15 in two different CCD modes, unbinned 1024×1024 CCD format in the nights with the best seeing and in binned 512×512 CCD format on the other nights.

2.2. Data Reduction

The raw data frames were processed following standard procedures to remove the bias, trim the pictures, and divide by mean sky flats obtained using color-balanced filters. No attempt was made to recover bad pixels or columns. We employed the image subtraction package ISIS V2.1 (Alard & Lupton 1998; Alard 2000) on these images. The resulting differential flux data produced light curves for a large number of variables. These stars were initially matched with those in the Clement et al. (2001) online catalog, and later as OT03 and ZK03 came out, with their newly discovered variables. In this analysis 13 new variables

were discovered. A later DAOPHOT/ALLFRAME analysis (Stetson 1994) on the same data resulted in better astrometry. An additional variable was detected in this analysis.

For the DAOPHOT/ALLFRAME analysis, the following procedure was used to determine the RA and Dec of the variable stars. Absolute equatorial coordinates (equinox J2000.0) for 11,738 stars within a $1^{\circ} \times 1^{\circ}25$ (E-W \times N-S) field centered on position $21^{\text{h}} 29^{\text{m}} 34^{\text{s}}.15 +11^{\circ} 59' 15''.0$ were selected from the USNO-A2.0 Guide Star database [Monet et al. 1998, USNO-A2.0 (Flagstaff: US Naval Obs.), CD-ROM] maintained by the Canadian Astronomy Data Centre. The equatorial coordinates were transformed to (ξ, η) rectangular coordinates measured in arcseconds relative to the reference position just given. At the same time, square $1^{\circ} \times 1^{\circ}$ images were extracted from the Digitized Sky Survey I “O” data and the DSS-II B , R , and I data, likewise through the services of the Canadian Astronomy Data Centre. Positions and magnitude indices for stars detected within these digitized Schmidt plates were obtained with a modernized version of the codes described in Stetson (1979a, 1979b). The program DAOMASTER was used to transform the photographic positions together with those from our CCD reductions to the (ξ, η) coordinate system defined by the USNO Guide Star catalog. From there, they could be transformed to the J2000.0 equatorial system of the USNO-A2.0 catalog. We anticipate that our absolute positions for *uncrowded*, well-exposed stars are accurately on the mean USNO-A2.0 system to well under $0''.1$, but positions of very faint stars or blended stars are likely to be more uncertain than this.

3. Periods and Light Curves

Table 1 gives the location of all the M15 variables found in this study in RA and Dec. The positions come from the research program described in Stetson (2000). Table 1 includes previously published periods when they exist and our newly determined periods.

The variable type is also given in Table 1.

Most of our data cover 7 days, spanning about 21 cycles for the shorter-period variables and about 10 cycles for the longer-period variables. There are a few additional data extending the time sequence to about 70 days. Because of the relatively short time interval of our data, periods are quoted to only 4 significant figures. Assuming we have correctly identified the variable, in several cases our period differs significantly from those previously published. In each case, the published period will not phase our data.

Table 2 gives the location of selected variables, primarily recent discoveries, generally toward the center of the cluster. In Table 2 we have converted RA and Dec coordinates to arcsec from the center of the cluster, as in the Sawyer-Hogg (1973, hereafter S-H) and the Clement et al. (2001) catalogs. The procedure we used for obtaining those values is as follows. Our coordinates in RA and Dec (as shown in Table 1) were converted to the S-H system by matching many of our variables with known variables from the catalog. The coordinates in OT03 are also given in RA and Dec. Similarly, these were converted to the S-H system by matching the previous known variables given at the top of their Table 4 with their corresponding values in the Clement catalog. The coordinates in ZK03 are given in the S-H system. ZK03 also provide corrected S-H coordinates for variables 128 through 155. Table 2 is intended to indicate the reliability of our identifications of previously known variables.

Periods were determined using the period-search program “kiwi,” which is based on the Lafler & Kinman (1965) algorithm. In other words, “kiwi” searches for periodicity by seeking to minimize the total length of the line segments that join adjacent observations in phase space, i.e., to maximize the smoothness of the light curve. (The “kiwi” program was kindly provided to us by Dr. Betty Blanco.)

Selected light curves based on our periods given in Table 1 are shown in Figures 1

and 2. Figure 1 includes some previously reported variables, but light curves for well established variables are not plotted. Figure 2 includes the variables reported for the first time in this paper. Most light curves are plotted in standard B magnitudes, while for some variables ISIS differential flux curves were used. In general, the light curves for a given star are smoother for the ISIS data than for the DAOPHOT/ALLFRAME data. The reason is that the ISIS reduction procedure consists of several steps. Initially, all the frames are transformed to a common coordinate grid. Next, a composite reference image is created by stacking several best seeing frames. For each frame, the composite reference image is convolved with a kernel to match its PSF and then subtracted. On the subtracted images, the constant stars cancel out, and only the signal from variable stars remains. A median image is constructed of all the subtracted images, and the variable stars are identified. Finally, profile photometry is extracted from the subtracted images. Thus, using ISIS we have obtained the relative fluxes for every variable star without contamination of the neighbor constant star companions and with much smoother, if any, sky background. Because of the standard magnitudes available in the DAOPHOT/ALLFRAME data, we chose to use these data for the figure whenever possible. ISIS data are used only for variables for which there were no DAOPHOT/ALLFRAME data or for which those data were extremely noisy. The internal precision of the photometry covers a wide range. For many stars the scatter about the mean loci is relatively small. For others it is barely sufficient to show that the star is in fact variable.

As already stated (§2.1), our data consist of images taken in two different formats. Nights with heliocentric Julian dates from 2452104 through 2452109 utilized a 512×512 CCD while night 2452110 and the later nights utilized a 1024×1024 CCD. Our initial image subtraction analysis utilized two different sets of reference frames, one BV set for each of the image formats. The fluxes are calculated with respect to these two different reference frames and as a result we have two different flux systems. In principle, it should be possible

to transform the relative fluxes to the instrumental magnitudes of the reference frames and thus to the standard system. The variables in the very crowded parts of the cluster, however, have no measured instrumental magnitudes. We also noticed some non-linearity in the transformation (see for example, Borissova et al. 2001). We then chose to rebin the original 512×512 images to 1024×1024 images. This allowed us to use a single B and a single V reference frame for the entire range of data. It is this analysis that is reported in this paper.

The comparison between original and rebinned data shows that the light curves of rebinned data are somewhat noisier. Since the rebinning conserves flux, there are two possible sources of noise. One is the difference between the real PSF and the very circular PSF which results from linearly interpolating the undersampled 512 images. The second is a much lower signal to noise ratio for the sky. However, having one single reference frame per filter allowed us to obtain a single differential flux light curve per filter for each variable star.

4. Standard Magnitudes and Light Curve Amplitudes

Using the light curves produced by the DAOPHOT/ALLFRAME analysis, the magnitude-averaged and intensity-averaged mean magnitudes of the variables were determined. These are shown in Table 3. Also shown in Table 3 are the BVI amplitudes. These were determined from measurements made on hardcopies of the light curves. As a check of the accuracy of this approach, we fitted some of the light curves with a high order polynomial function and calculated the amplitude of the variable. The error in amplitude was determined by adding in quadrature the standard deviation of the light curve fit at maximum and minimum light. These calculations indicate that the errors of the amplitudes are within 0.01 to 0.03 mags. For the light curves that were very noisy, including many of

the suspected double-mode pulsators, no amplitudes are given.

Figure 3 is a histogram of the M15 RR Lyrae periods with the RRab (or RR0) and RRc (RR1) variables clearly separated. For the purposes of this figure, the suspected RRd (RR01) variables have been grouped with the RRc variables. The RRc variables (including possible RRd variables) all have periods less than 0.45 d while the RRab variables all have periods greater than 0.55 d. The average period for the 68 stars that are very likely RRab variables is 0.644 d and for the 95 stars that are very likely RRc (or RRd) variables is 0.370 d. Figure 4 is similar to Figure 3 except that the periods of the RRc (and possible RRd) variables have been fundamentalized by adding 0.128 to their log period. As can clearly be seen from this plot, the fundamentalized period distribution presents a clear peak at a value $P_f \simeq 0.53$ d. A secondary “hump” is also hinted at, located at $P_f \simeq 0.67$ d. Both these features were previously noted and discussed in Catelan (2004), who points out that neither of these features is predicted by canonical stellar evolution/pulsation theory. In particular, such peaked distributions appear especially difficult to account for in terms of the evolutionary paradigm for the origin of OoII clusters, according to which RR Lyrae variables in the latter are evolved away from a position on the blue zero-age HB. Indeed, the average period of the RRab variables (0.644 d), the average periods of the RRc variables (0.370 d), the number fraction of c-types (1.40), and the minimum period of the RRab-type variables (0.55380 d) all consistently indicate an OoII type for the cluster. As recently shown by Catelan et al. (2007), $\langle P_{ab} \rangle$ and $P_{ab, \min}$ are particularly reliable indicators of Oosterhoff type.

It is somewhat surprising, therefore, that M15’s RRab stars do not appear to follow the same trend as do RRab stars in other globular clusters, as far as the Bailey diagram is concerned. This is shown in Figure 5, which provides a plot of B amplitude as a function of log period. As has long been known, for the RRab variables, the amplitude decreases

as the period increases, while for the RRc variables, the amplitude first increases and then decreases with increasing period (Sandage 1981a). Also shown in the Figure are typical lines for the RRab variables in Oo II and Oo I clusters. These were taken from Cacciari, Corwin, & Carney (2005). Figure 6 is a plot of V amplitudes as a function of log period. As can clearly be seen, there are many stars in the cluster occupying an intermediate position in the Bailey diagram between OoI and OoII, and even some that better match the OoI locus. This has been seen before for M15, for instance in Figure 4 of Cacciari et al. 2005. Also, as shown by Pritzl et al. (2002), there is indeed no a priori reason why all stars in all Oo II globular clusters should fall precisely on the same line (see their Fig. 16), so that the apparent “Oosterhoff-intermediate” nature of M15 in the Bailey diagrams of Figures 5 and 6 may in fact reveal more a deficiency of the latter in correctly identifying Oosterhoff status than an actual intermediate status for the (prototypical!) type II globular cluster M15—a cluster which, as already stated, completely lacks RRab variables with periods shorter than 0.55 d, which happens to be the typical *average* RRab period in OoI globular clusters (e.g., Smith 1995; Clement et al. 2001; Catelan 2007).

A factor that would affect the location of RR Lyrae stars in the Bailey diagram is the presence of blended stars in the data. Blended stars have lower amplitudes for a given period. In these cases, a plot with the correct (unblended) amplitude would move the variable up in the diagram, in the direction of the typical line for OoII clusters. A blend with a star of different color (which in general one would expect to be the case) would also affect the ratio of the B and V amplitudes. To look for this effect, we plotted the ratio of A_B/A_V against V magnitude (see Figure 7). However, in the figure there appears to be very little difference in the amplitude ratios of the brighter and the fainter stars. Higher resolution images of M15 taken with the *HubbleSpaceTelescope* (to be discussed in Paper II) have the potential to reveal near neighbor stars that might go undetected in observations made from the ground. However, inspection of HST images of M15 did not

reveal a significant number of likely blends. At this time, we have no clear explanation for the period shift spread in the M15 RRab variables.

The location of an RRab variable in the period-amplitude plane of Figure 5 is a measure of its average luminosity, which is determined by its surface temperature and radius (the Stefan-Boltzmann equation). Sandage (1981a, 1981b), Jones et al. (1992), Catelan (1998), and Sandquist (2000) have shown that the B amplitude of an RRab variable is related to its effective temperature; the larger the amplitude, for a given metallicity, the higher the temperature (but see De Santis 2001). The pulsation equation relates the period of a variable star to its average density; the period is inversely proportional to the square root of the average density. Assuming that the masses of the variables are distributed in a narrow range, the period becomes a measure of the average size of the star; the longer the period, the larger the star. Thus, for a given amplitude (temperature), the longer period (larger) variables should be more luminous. Assuming all of the variables are cluster members and thus at about the same distance, the position of a variable in the period-amplitude plane should correspond to its apparent brightness.

When computing evolutionary models, it is much easier to provide as an output the stellar equilibrium temperature than the pulsation amplitude, given that the latter can only be computed on the basis of complex non-linear pulsation models, whereas the former is directly provided as output in any standard stellar evolution code. Therefore, period shifts (with respect to some convenient reference line) *at fixed temperature* are routinely computed when synthetic HB models are produced (see, e.g., Lee, Demarque, & Zinn 1990; Pritzl et al. 2002). Observers, on the other hand, generally compute period shifts *at fixed amplitude*. If amplitude is a good indicator of temperature, then the two diagrams are fairly equivalent, and the period shifts computed by modelers and observers can be directly compared.

V171 with a period of about 0.55 d and an amplitude of only 0.84 mag in B occupies

an unusual position in Figure 5. A possible explanation is that, as its period might suggest, it is a double-mode variable (0.55 d is the approximate fundamental period for M15 double-mode pulsators). A period of 0.3547 d does phase the data well, but this period is not at the proper ratio for the first-overtone period. Also, the plot at this period strongly resembles that of a fundamental pulsator. If V171 is, in fact, a double-mode pulsator, it appears as if the primary mode of pulsation is the fundamental mode, which would be unusual. Another possibility is that it is a Blazhko variable pulsating at less than maximum amplitude as discussed below.

In general, the expectation that the brighter RR Lyraes should fall closer to the OoII line in the Bailey diagram and that the dimmer ones should fall closer to the OoI line is confirmed in Figure 5. The 9 variables closest to the OoI line have $\langle B \rangle = 16.262$, although there are 2 anomalies, V77 at $\langle B \rangle = 16.118$ and V163 at $\langle B \rangle = 16.043$, the brightest RRab in our data. The 11 variables closest to the OoII line have $\langle B \rangle = 16.182$. There are 7 variables that lie well to the right of the OoII line in Figure 5. They are V9, V19, V20, V47, V49, V55, and V162. V9, V19, V47, and V162 are relative bright with $\langle B \rangle = 16.168$. However, V20, V49, and V55 are relative faint with $\langle B \rangle = 16.277$.

There are a number of explanations for why the luminosity indicated by the position of a variable on the Bailey diagram does not correspond to its apparent magnitude. As discussed above, if the star is a blended star, it will appear brighter than its pulsational properties indicate. If the star is not a member of the cluster, but is at a greater or lesser distance, its pulsational properties will not correspond to its apparent brightness. Ratnatunga & Bahcall (1985) indicate an expected 0.1 field stars with $B - V \leq 0.8$ per square arcminute near the horizontal branch. The “Rozhen” images cover an area of about 32 square arcminutes, so we might expect 3 or 4 interloping field stars.

Another factor that might result in the location of the variable on the Bailey diagram

not correctly representing is apparent brightness is the Blazhko effect. For the RRab variables in Figures 6 and 7, there is considerable scatter. Clement & Shelton (1999) pointed out that Blazhko variables introduce scatter into the period-amplitude diagram. This is because the Clement & Shelton period-amplitude relations for OoI and OoII variables only apply when they are at maximum amplitude. The scatter is introduced when the light curve of a Blazhko variable represents it at less than its maximum amplitude. Additional intrinsic scatter can also be present as a consequence of RR Lyrae stars being in different evolutionary stages (see Pritzl et al. 2002 for a discussion).

5. Notes On Individual Stars

V39 — As seen from the light curve in Figure 1, 0.38955 d does not phase the data well. In M15 double-mode pulsators have first-overtone periods of about 0.4 d and fundamental-mode periods of about 0.55 d. Thus, V39 may be a double-mode pulsator. There have been many variables previously identified as double-mode pulsators and many new candidates in our data. However, our data are not adequate to firmly constrain secondary periods for suspected double-mode RR Lyrae.

V139 — This variable and ZK44 are separated by only 1.15 arcsec. Table 1 assumes V139 and ZK44 are the same variable, though this might not be the case. Our period differs from the one in OT03. However, our data are limited and it is not clear that our period is correct.

V159 — In OT03 this variable is listed as a combination of three variables.

V160 — This variable and ZK52 are separated by only 0.37 arcsec. Table 1 assumes that these are the same variable.

V161 — This variable and ZK39 are separated by only 0.05 arcsec. Table 1 assumes

that these are the same variable.

V162 — This variable and ZK18 are separated by only 0.71 arcsec. Table 1 assumes that these are the same variable.

V164 — This variable and ZK37 are separated by only 0.11 arcsec. Table 1 assumes that these are the same variable. OT03 give a period of 0.4275 d while ZK03 suggest that ZK37 may be a second overtone pulsator. The star we located is 0.66 arcsec from ZK37 and 0.75 arcsec from V164. Although our star appears to be variable, we could not determine a period that phased the data well.

V165 — This variable and ZK32 are separated by only 0.03 arcsec. Table 1 assumes that these are the same variable. OT03 give a period of 0.4339 d while ZK03 do not attempt to identify the variable type for ZK32. The variable we located is 0.11 arcsec from V165 and 0.18 arcsec from ZK32. Our period differs from the one in OT03. However, our data are limited and it is not clear that our period is correct.

V166 — This variable and ZK22 are separated by only 0.49 arcsec. Table 1 assumes that these are the same variable.

V169 — This variable and ZK23 are separated by only 0.41 arcsec. Table 1 assumes that these are the same variable.

V172 — This variable and ZK13 are separated by only 0.93 arcsec. Table 1 assumes that these are the same variable.

V173 — This variable and ZK11 are separated by only 0.96 arcsec. Table 1 assumes that these are the same variable.

V174 — This variable and ZK10 are separated by only 0.93 arcsec. Table 1 assumes that these are the same variable.

V175 — This variable and ZK6 are separated by only 1.19 arcsec. Table 1 assumes that these are the same variable.

V177 — This variable and ZK64 are separated by only 0.66 arcsec. Table 1 assumes that these are the same variable.

V178 — This variable and ZK55 are separated by only 0.59 arcsec. Table 1 assumes that these are the same variable. OT03 give a period of 0.2860 d while ZK03 suggest that ZK37 may be a second-overtone pulsator. However, the OT03 period does not phase our data well. Our best period is 0.3983 d, with the light curve suggesting a double-mode pulsator.

V181 — This variable and ZK14 are separated by only 0.63 arcsec. Table 1 assumes that these are the same variable. OT03 give a period of 0.5868 d. Our best period is 0.40097 d. These periods suggest that V181 is a double-mode pulsator.

ZK34 — ZK03 suggest that this variable may be a second overtone pulsator. Our period of 0.29765 d could be consistent with this.

ZK62 — We did locate a star within 0.59 arcsec of this variable. Our data were very noisy, but did produce a slight periodic brightening at about 0.05 d.

ZK74 — This star has a very unusual light curve for a period of 0.3195 d. ZK03 indicate that this star may be an RRab variable. However, no longer period would properly phase our data.

NV14 — Our variable is 3.4 arcsec from the Clement Catalog coordinates for V109. We assume we did not detect V109 and that our star is a new variable.

For the following stars, our data suggest variability, but no period could be determined from our data: V108, V109, V110, V112, V115, V116, V137, V146, V147, V148, V149,

V150, V153, V164, ZK3, ZK44, ZK47, and ZK62.

6. Summary

In this paper, we have presented new *BVI* CCD photometry for variable stars in the globular cluster M15. Our photometry was obtained with both the image subtraction package ISIS (Alard 2000) and with DAOPHOT/ALLFRAME (Stetson 1994). Our analysis has led to the first period determinations for 40 previously known variables. Improved periods were also obtained for 67 previously known variables, and 14 new variables were discovered in the course of our study. Our results bring the grand total of M15 RR Lyrae variables to $N_{\text{RR}} = 194$, implying a specific RR Lyrae fraction of $S_{\text{RR}} = N_{\text{RR}} \times 10^{0.4(7.5+M_V)} = 41.7$ (for an absolute magnitude of the cluster $M_V = -9.17$ Harris 1996), compared with the value 18.9 as given in the 2003 edition of the Harris (1996) catalog.

We warmly thank H. Markov for the observations carried out in September 2001. Support for M.C. was provided by Proyecto FONDECYT Regular No. 1071002. HAS thanks the National Science Foundation for support under grant AST 0607249. J.B. is supported by Fondap Center for Astrophysics 15010003 and received partial support from Centro de Astrofísica de Valparaíso, Universidad de Valparaíso.

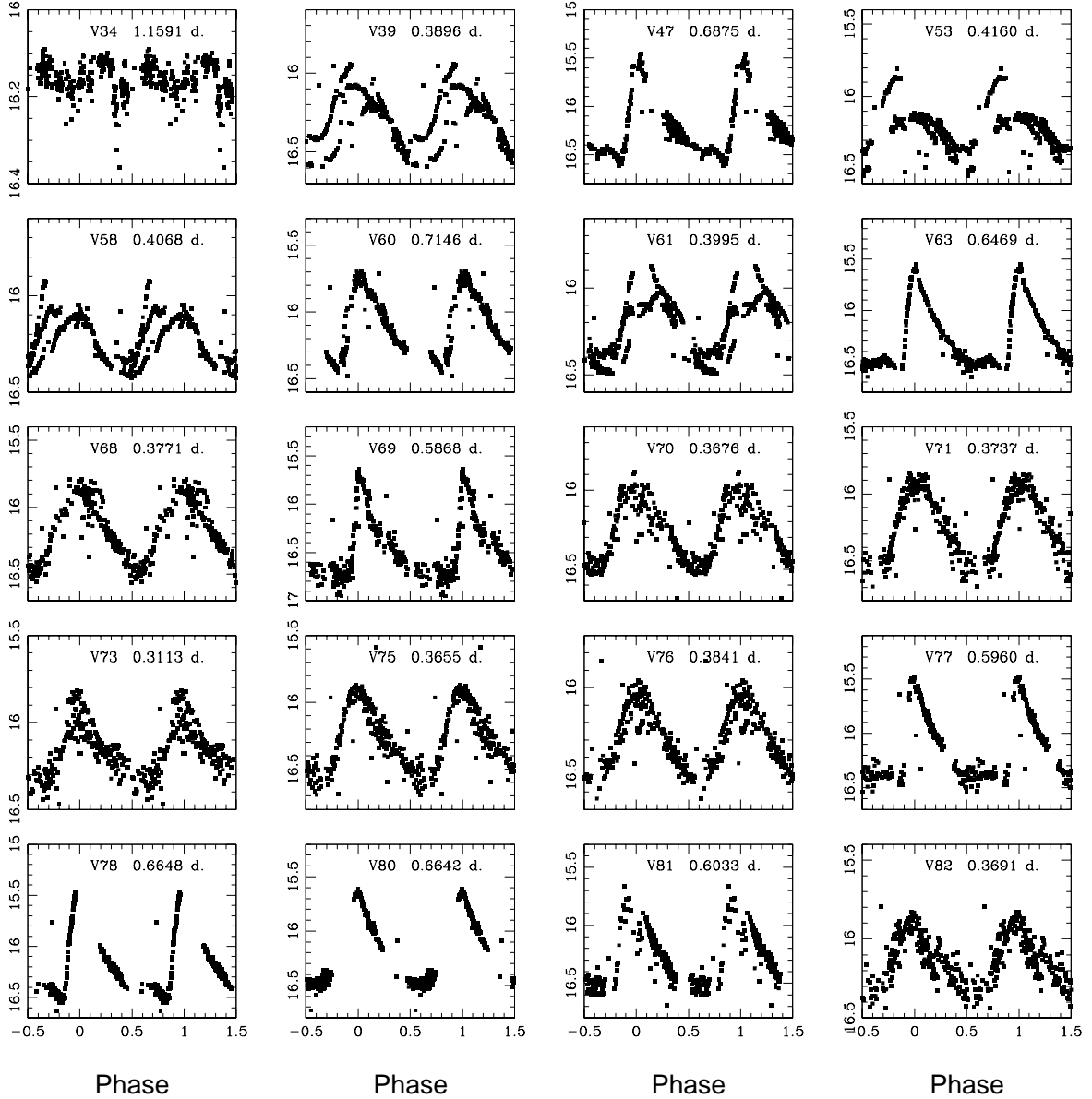


Fig. 1.— *B* light curves for selected previously identified variable stars in M15. ISIS data are plotted in arbitrary units and values are not listed on the y axes. DAOPHOT/ALLFRAME data are plotted in standard magnitudes.

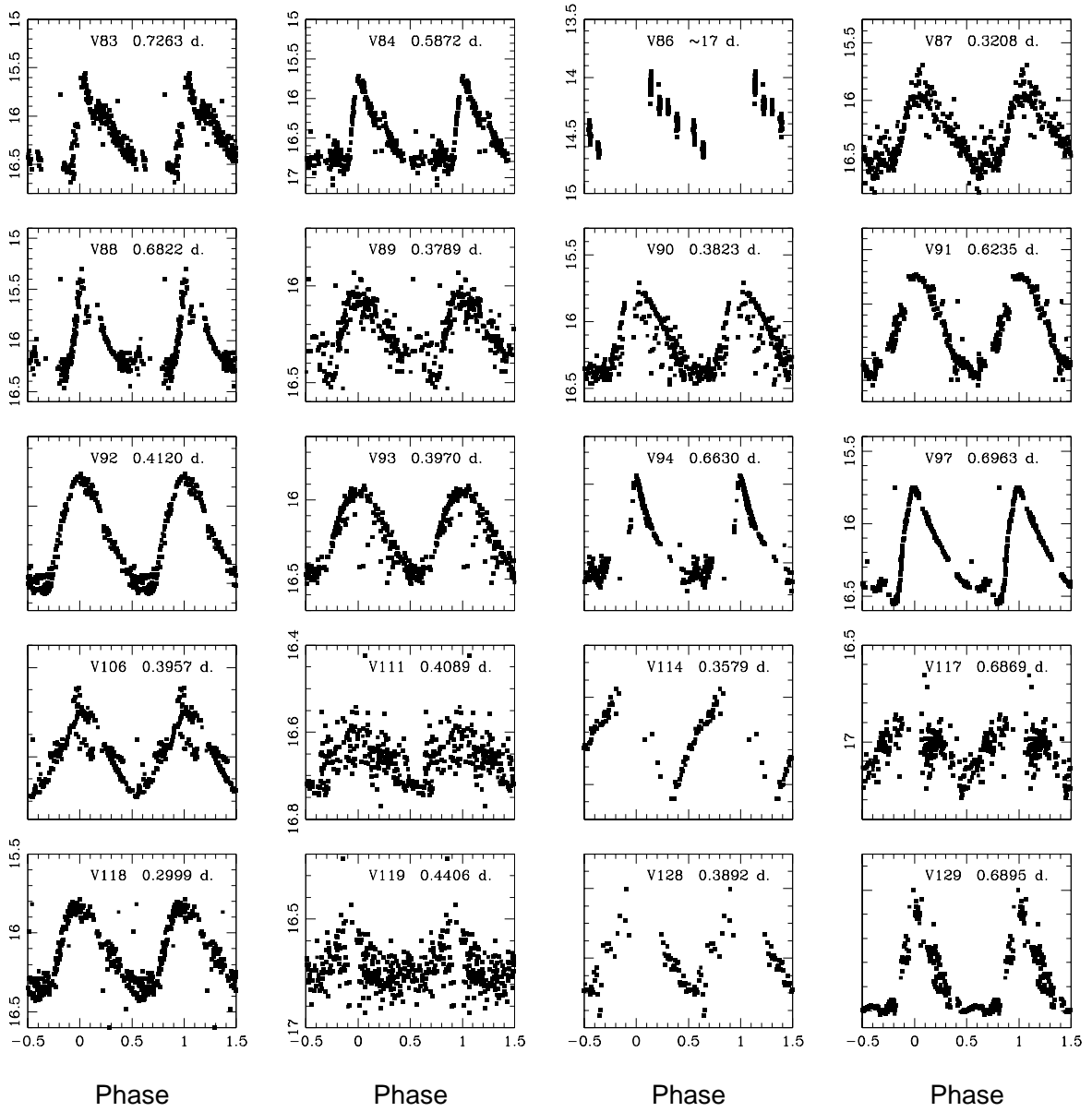


Fig. 1 (*continued*).—

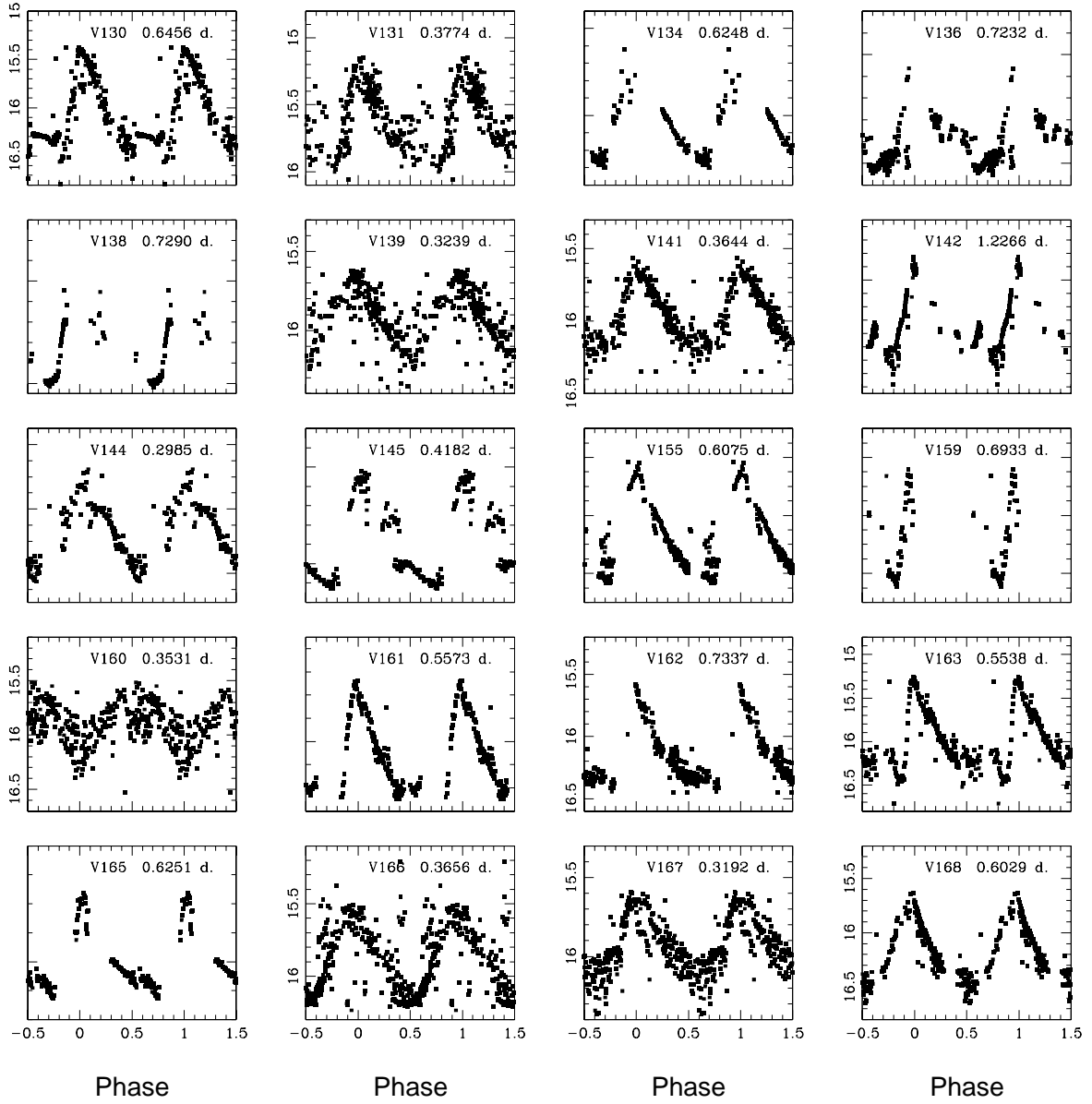


Fig. 1 (*continued*).—

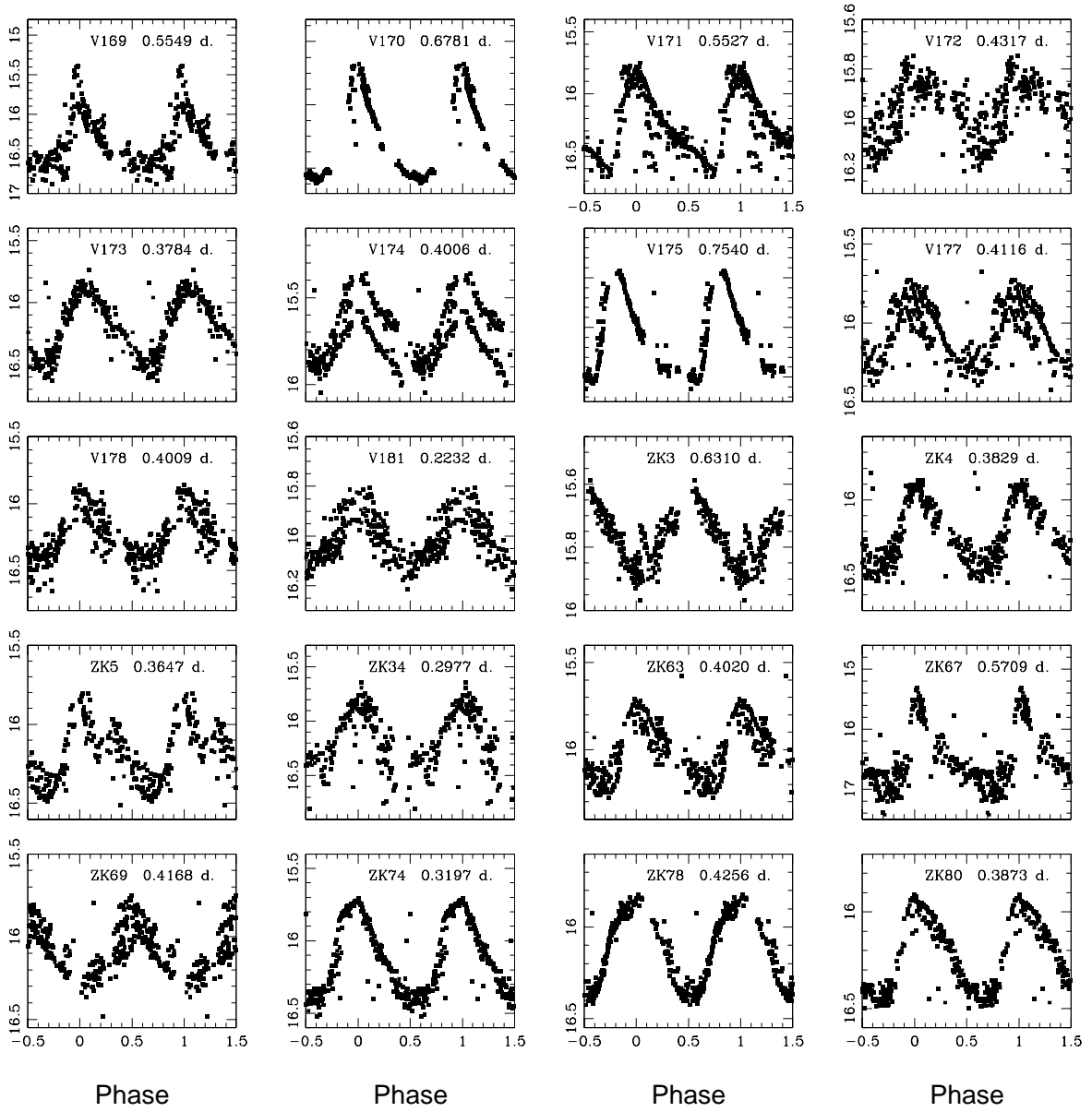


Fig. 1 (*continued*).—

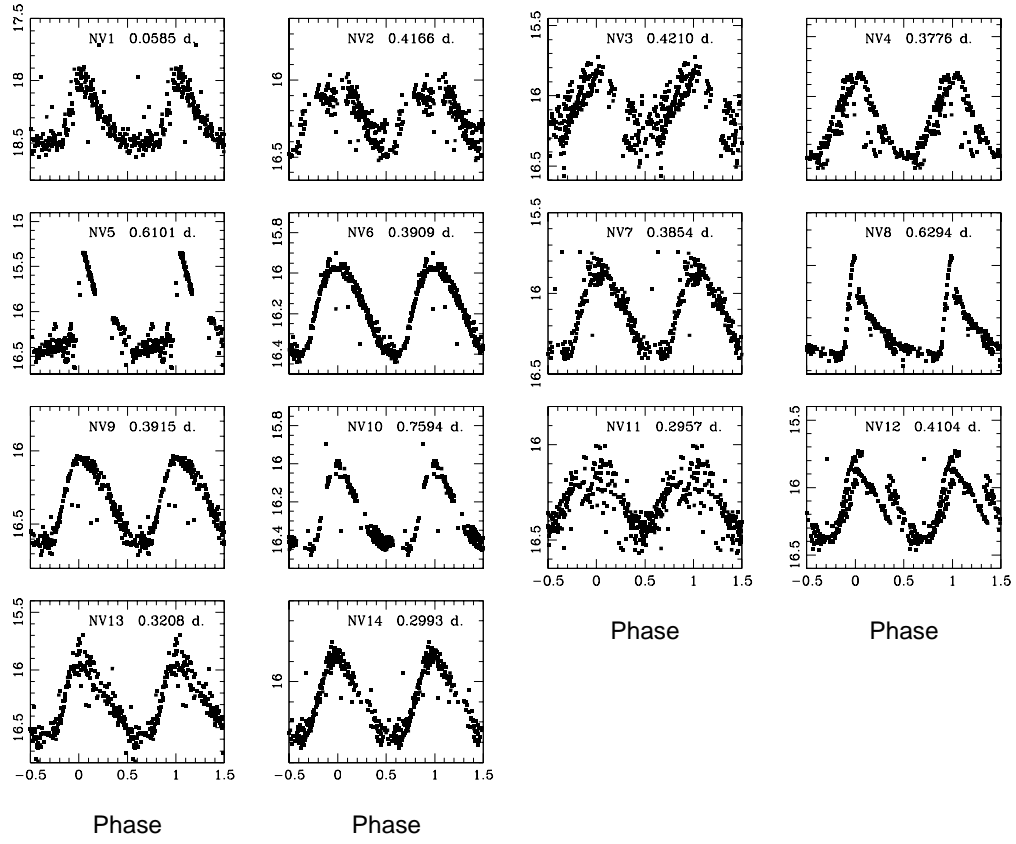


Fig. 2.— *B* light curves for the newly discovered variable stars in M15. ISIS data are plotted in arbitrary units while DAOPHOT/ALLFRAME data are plotted in standard magnitudes.

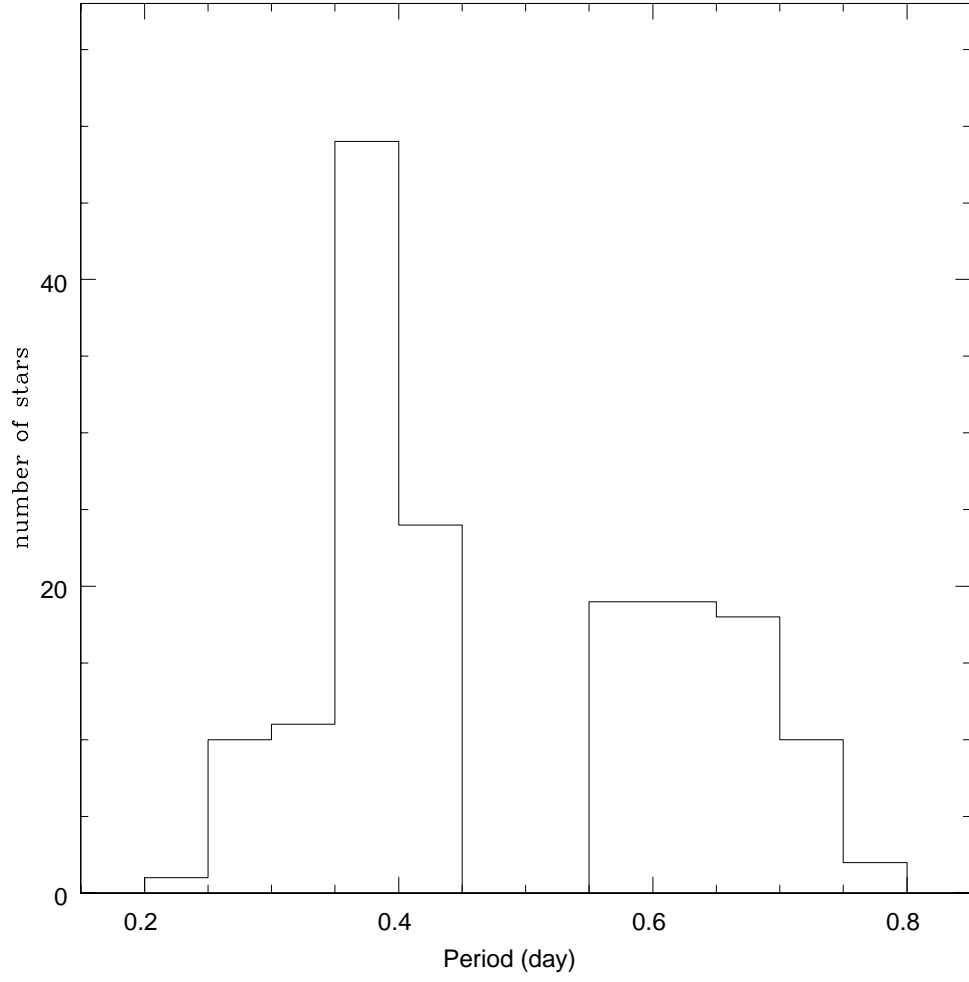


Fig. 3.— Histogram of the periods of M15 variables.

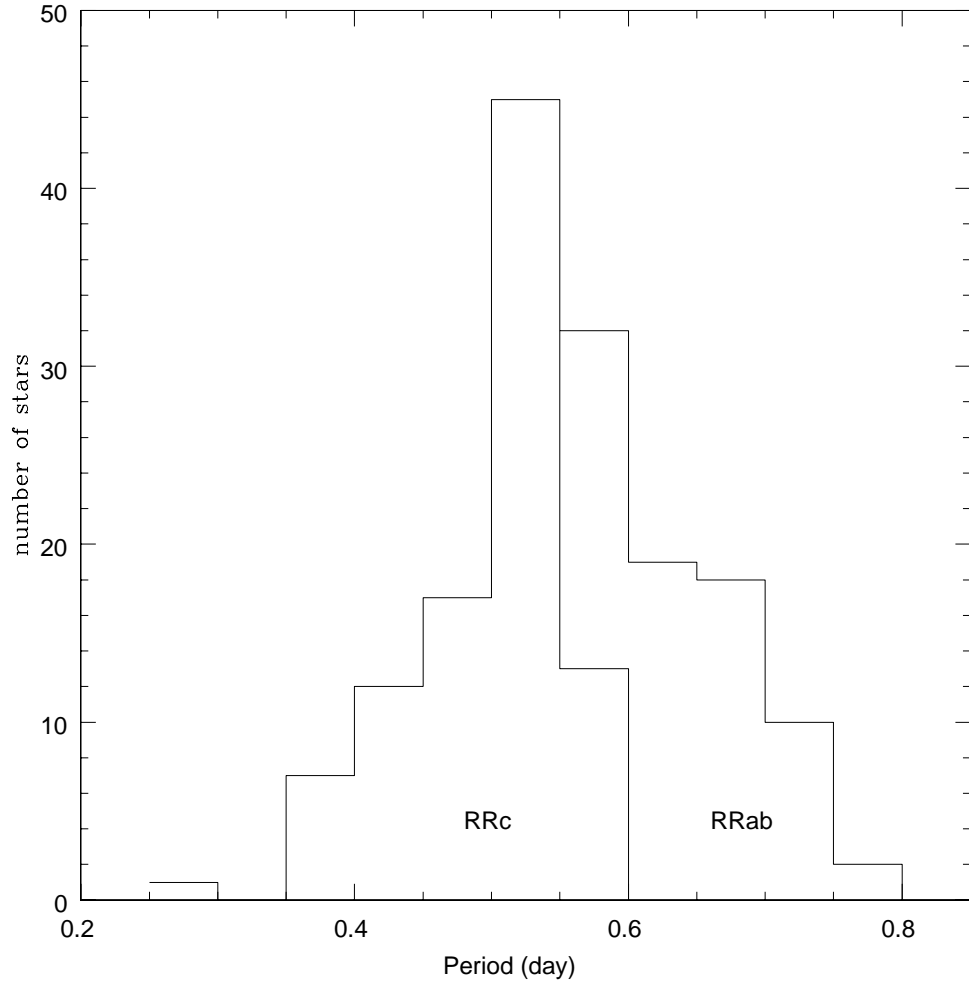


Fig. 4.— Histogram of the fundamentalized periods of M15 variables.

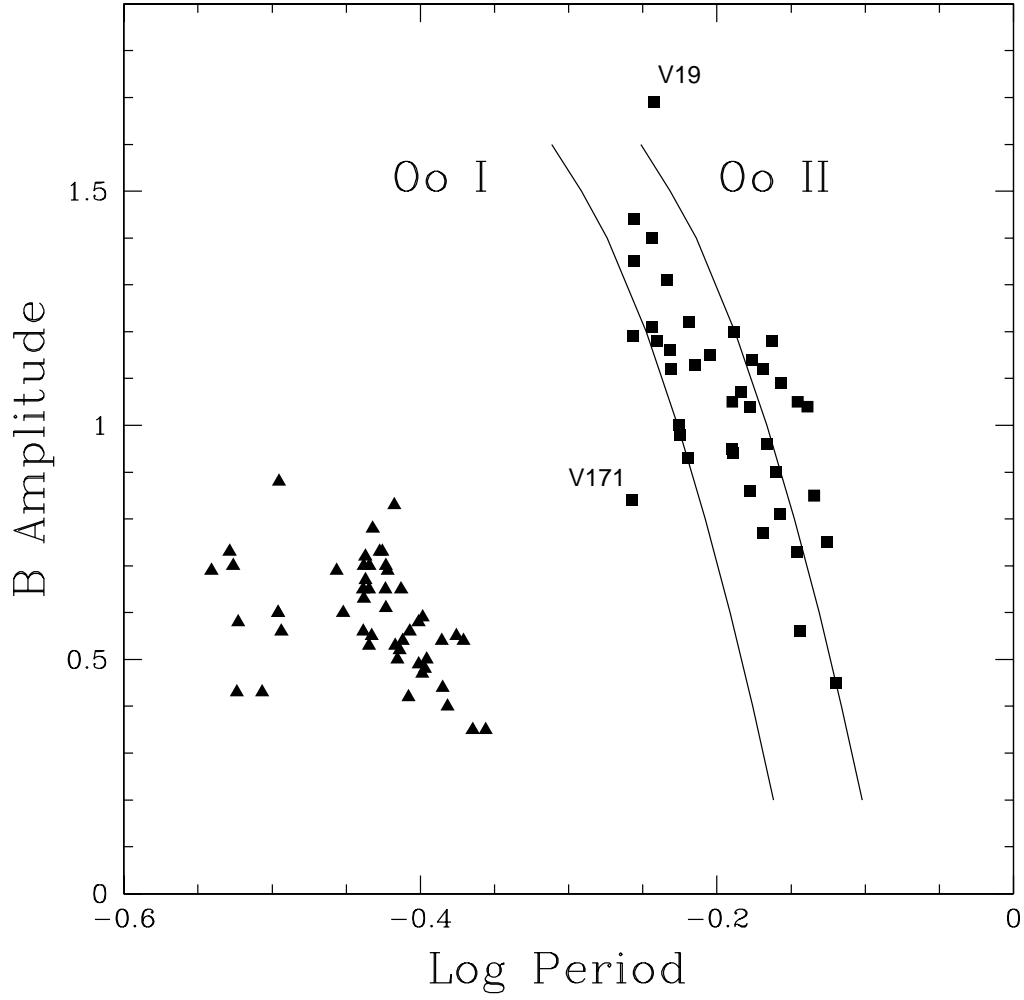


Fig. 5.— B amplitude vs log period (days). Filled triangles for RRc and filled squares for RRab.

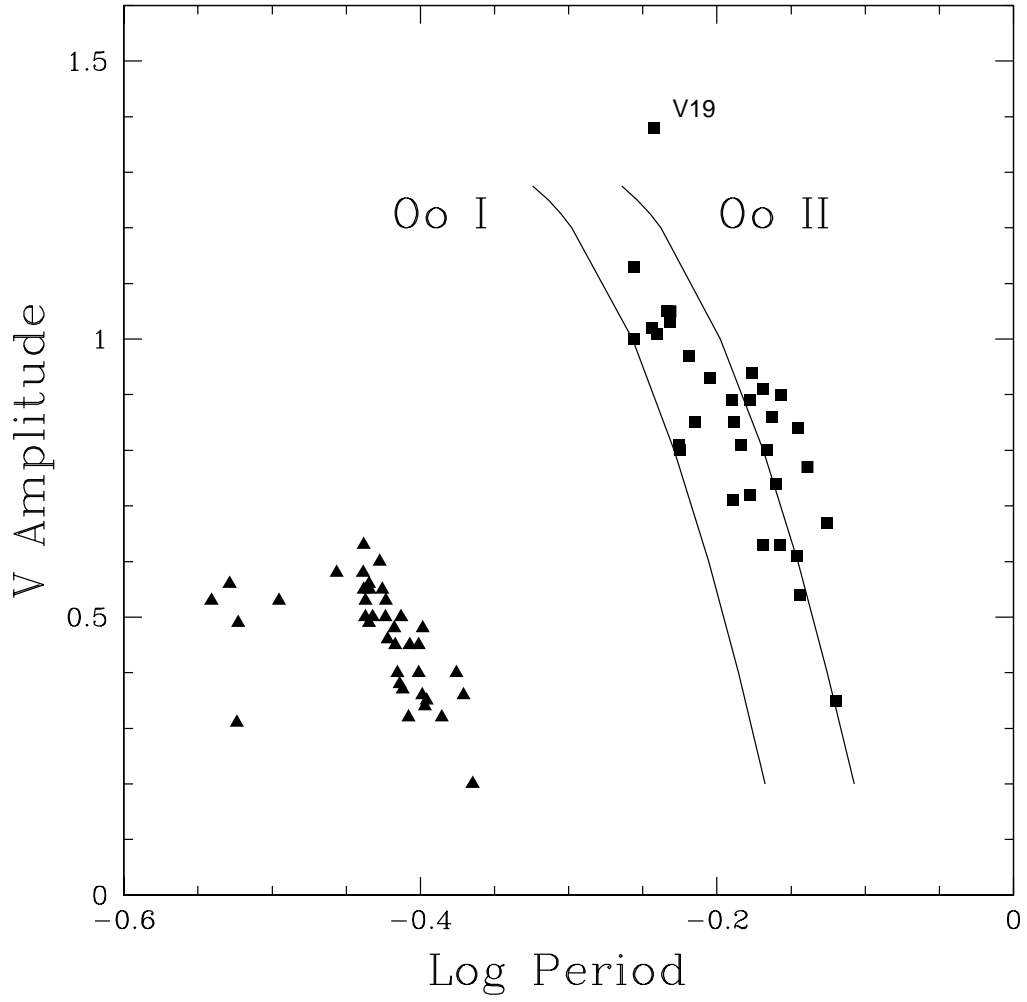


Fig. 6.— V amplitudes vs. log period (symbols as in Figure 5).

REFERENCES

- Alard, C. 2000, *A&AS*, 144, 235
- Alard, C. & Lupton, R. H. 1998, *ApJ*, 503, 325
- Arellano, F. A., Garcia Lugo, G. & Rosenzweig, P. 2006, *RMxAA*, 42, 75
- Bingham, E. A., Cacciari, C., Dickens, B. J., Pecci, F. F. 1984. *MNRAS*, 209, 765
- Butler, R. F., Shearer, A., Redfern, R. M., et al. 1998, *MNRAS*, 296, 379
- Cacciari, C., Corwin, T. M., & Carney, B. W. 2005, *AJ*, 129, 267
- Carney, B. W. 2001, in *Star Clusters*, ed. L. Labhardt & B. Binggeli (Berlin: Springer), 1
- Catelan, M. 1998, *ApJ*, 495, 81
- Catelan, M. 2004, *ApJ*, 600, 409
- Catelan, M. 2007, in *Resolved Stellar Populations*, ed. D. Valls-Gabaud & M. Chávez, in press (astro-ph/0507464)
- Catelan, M., Greco, C., Clementini, G., Smith, H. A., De Lee, N., Pritzl, B. J., Rest, A., Held, E. V., & Poretti, E. 2007, in preparation
- Clement, C. M., Muzzin, A., Dufton, Q., et al. 2001, *AJ*, 122, 2587
- Clement, C., & Shelton, I. 1999, *ApJ*, 515, L85
- De Santis, R. 2001, *MNRAS*, 326, 397
- Harris, W. E. 1996, *AJ*, 112, 1487
- Harris, W. E. 2001, in *Star Clusters*, ed. L. Labhardt & B. Binggeli (Berlin: Springer), 223
- Jones, R. V., Carney, B. W., Storm, J., & Latham, D. W. 1992, *ApJ*, 386, 646
- Lafler, J. & Kinman, T. D. 1965, *ApJS*, 11, 216L
- Lee, Y.-W., Demarque, P., & Zinn, R. 1990, *ApJ*, 350, 155

- Monet, D. G., et al. 1998, USNO-A2.0 (Flagstaff: US Naval Obs.), CD-ROM
- Oosterhoff, P. Th. 1939, *Observatory*, 62, 104
- Ó Tuairisg, S. O., Butler, R. F., Shearer, A., Redfern, R. M., Butler, D., & Penny, A. 2003, *MNRAS*, 345, 960 (OT03)
- Pritzl, B. J., Smith, H. A., Catelan, M., & Sweigart, A. V. 2002, *AJ*, 124, 949; erratum: *AJ*, 125, 2752
- Ratnatunga, K. U. & Bahcall, J. N. 1985, *ApJs*, 59, 63
- Sandage, A. 1981a, *ApJ*, 244, L23
- Sandage, A. 1981b, *ApJ*, 248, 161
- Sandage, A. Katem, B., & Sandage, M. 1981, *ApJS*, 46, 41
- Sandquist, E. L. 2000, *MNRAS*, 313, 571
- Sawyer Hogg, H. 1973, *Publ. David Dunlap Obs*, 3, 6
- Silbermann, N. A. & Smith, H. A. 1995, *AJ*, 110, 704
- Smith, H. A. 1995, *RR Lyrae Stars* (Cambridge: Cambridge Univ. Press)
- Sosin, C & King, I. R. 1997, *AJ*, 113, 1328
- Stetson, P. B. 1979a, *AJ*, 84, 1056
- Stetson, P. B. 1979b, *AJ*, 84, 1149
- Stetson, P. B. 1994, *PASP*, 106, 250
- Stetson, P. B. 2000, *PASP*, 112, 925
- Zheleznyak, A. P. & Kravtsov, V. V. 2003, *AstL*, 29, 599 (ZK03)

Table 1. M15 Variables

Variable	RA h m s	Dec ° ' "	Previous period (d)	Our Period (d)	Type
V1	21 29 50.20	12 10 26.9	1.437712	1.4378	Ceph?
V6	21 29 59.92	12 11 19.8	0.665967	0.6660	RR0
V7	21 29 58.98	12 11 16.8	0.367557	0.367557	RR1
V8	21 29 58.22	12 12 10.2	0.64625	0.6462	RR0
V9	21 29 59.24	12 12 21.9	0.715295	0.715295	RR0
V10	21 30 06.85	12 10 05.5	0.386382	0.386382	RR01?
V13	21 30 06.95	12 08 55.3	0.57491	0.57491	RR0
V16	21 30 05.09	12 12 13.2	0.3992	0.3992	RR01?
V17	21 30 03.95	12 11 53.6	0.428907	0.4294	RR01
V18	21 30 03.53	12 11 44.1	0.367737	0.367737	RR1
V19	21 30 05.81	12 12 44.2	0.57228	0.5723	RR0
V20	21 30 03.79	12 09 53.8	0.697021	0.697021	RR0
V21	21 30 00.60	12 09 05.5	0.6488	0.6476	RR0
V24	21 29 51.01	12 09 56.1	0.369693	0.3697	RR1
V32	21 29 54.79	12 11 50.2	0.60547	0.6044	RR0
V33	21 29 55.51	12 09 34.1	0.5839452	0.5839452	RR0
V34	21 29 54.53	12 09 07.5	none	1.1591	EB?
V36	21 29 56.42	12 08 41.6	0.624151	0.624151	RR0
V37	21 29 56.58	12 08 45.6	0.28775	0.28775	RR1
V38	21 29 58.85	12 07 36.9	0.375265	0.375265	RR1

Table 1—Continued

Variable	RA h m s	Dec ° ' "	Previous period (d)	Our Period (d)	Type
V39	21 29 59.71	12 07 58.7	0.389563	0.389563	RR01
V40	21 30 07.27	12 08 07.1	0.37735	0.3777	RR1
V41	21 30 02.61	12 09 08.4	0.382177	0.382177	RR01
V44	21 30 04.49	12 10 07.2	0.59558	0.5945	RR0
V45	21 30 02.83	12 09 32.1	0.677399	0.677399	RR0
V46	21 30 02.20	12 10 35.7	0.691466	0.691466	RR0
V47	21 30 01.28	12 09 59.6	0.602799	0.6875	RR0
V48	21 30 02.29	12 12 33.8	0.364971	0.3646	RR1
V49	21 30 00.95	12 12 49.3	0.65518	0.65518	RR0
V50	21 30 09.44	12 11 44.0	0.29806	0.29806	RR01
V51	21 29 58.67	12 11 34.4	0.396935	0.396935	RR01
V53	21 29 52.05	12 08 11.9	0.414096	0.4160	RR01
V54	21 29 59.00	12 11 31.4	0.399568	0.399568	RR01
V55	21 30 02.76	12 09 44.7	0.748596	0.7486	RR0
V56	21 30 02.17	12 10 03.9	0.5704	0.5703	RR0
V57	21 30 03.40	12 09 08.6	0.537481	0.3496	RR1
V58	21 29 54.50	12 10 11.4	0.407685	0.4068	RR01
V59	21 30 01.07	12 10 45.7	0.554792	0.5546	RR0
V60	21 30 01.93	12 09 04.3	0.73124	0.7146	RR0
V61	21 29 53.73	12 09 21.4	0.39881	0.3995	RR01

Table 1—Continued

Variable	RA	Dec	Previous period	Our Period	Type
	h m s	° ' "	(d)	(d)	
V62	21 29 53.41	12 10 41.4	0.3773	0.3773	RR01
V63	21 30 01.59	12 10 34.2	0.68332	0.6469	RR0
V64	21 29 55.13	12 10 22.6	0.3642	0.3642	RR1
V65	21 29 51.33	12 09 24.2	0.718196	0.7182	RR0
V66	21 29 53.65	12 08 10.6	0.37935	0.37935	RR1
V67	21 29 52.40	12 09 52.5	0.404627	0.4064	RR01?
V68	21 29 56.13	12 10 15.3	none	0.3771	RR1
V69	21 29 55.79	12 09 37.2	none	0.5868	RR0
V70	21 29 55.98	12 09 43.6	none	0.3676	RR1
V71	21 29 55.94	12 09 50.4	none	0.3737	RR1
V73	21 29 58.04	12 10 23.2	none	0.3113	RR1
V74	21 30 00.90	12 08 37.7	0.29601	0.29601	RR1
V75	21 29 58.47	12 09 32.1	none	0.3655	RR1
V76	21 29 58.37	12 09 34.3	none	0.3841	RR1
V77	21 29 57.57	12 09 40.5	none	0.5960	RR0
V78	21 29 57.83	12 10 50.6	0.398879	0.6648	RR0
V80	21 29 55.08	12 09 36.2	none	0.6642	RR0
V81	21 29 56.83	12 09 57.9	none	0.6033	RR0
V82	21 29 56.88	12 10 04.9	none	0.3691	RR1
V83	21 29 59.39	12 09 56.8	none	0.7263	RR0

Table 1—Continued

Variable	RA h m s	Dec ° ' "	Previous period (d)	Our Period (d)	Type
V84	21 29 59.51	12 09 48.9	none	0.5872	RR0
V86	21 29 59.18	12 10 07.5	17.109	?	Ceph?
V87	21 30 00.03	12 09 39.3	none	0.3208	RR1
V88	21 29 58.43	12 10 29.6	none	0.6822	RR0
V89	21 29 56.70	12 09 55.8	none	0.3789	RR1
V90	21 30 00.48	12 10 07.8	none	0.3823	RR1
V91	21 30 02.89	12 10 31.1	none	0.6235	RR0
V92	21 29 59.00	12 09 37.8	none	0.4120	RR1
V93	21 30 00.30	12 09 29.5	none	0.3970	RR01
V94	21 29 58.48	12 10 31.4	none	0.6630	RR0
V97	21 29 52.87	12 10 31.8	0.696336	0.696336	RR0
V106	21 29 56.13	12 10 17.0	none	0.3957	RR01
V111	21 30 01.20	12 10 03.3	none	0.4089	RR01
V114	21 29 58.19	12 10 53.3	none	0.3579	RR1
V117	21 29 59.31	12 09 27.3	none	0.6869	RR0
V118	21 29 59.63	12 10 56.0	none	0.3000	RR01
V119	21 29 59.65	12 10 07.6	none	0.4406	RR1
V128	21 29 58.41	12 10 02.3	0.4034	0.3892	RR01?
V129	21 29 57.85	12 09 49.0	0.6876	0.6895	RR0
V130	21 29 57.87	12 09 52.3	0.652	0.6456	RR0

Table 1—Continued

Variable	RA h m s	Dec ° ' "	Previous period (d)	Our Period (d)	Type
V131	21 29 57.86	12 10 00.8	0.5994	0.3774	RR1?
V132	21 29 57.85	12 10 03.0	0.3930	0.4002	RR01
V134	21 29 58.03	12 09 59.3	0.3828	0.6248	RR0
V136	21 29 58.18	12 10 07.3	0.7069	0.7232	RR0
V137	21 29 58.29	12 10 05.6	0.3520	0.5388	RR1
V138	21 29 58.48	12 10 00.9	0.7143	0.7290	RR0
V139	21 29 58.43	12 10 11.5	0.3258	0.3239	RR1
V141	21 29 58.97	12 10 03.6	0.3644	0.3644	RR1
V142	21 29 58.60	12 10 01.0	1.2411	1.2266	Ceph?
V144	21 29 59.30	12 10 01.4	0.299	0.2985	RR1
V145	21 29 59.34	12 10 03.2	0.4224	0.4182	RR01?
V159	21 29 58.35	12 10 02.6	0.6385	0.6933	RR0
V160	21 29 58.10	12 09 48.6	0.3529	0.3531	RR1
V161	21 29 58.51	12 09 49.5	1.2773	0.5573	RR0
V162	21 29 59.55	12 09 50.0	0.7299	0.7337	RR0
V163	21 29 59.25	12 09 52.3	0.5601	0.5538	RR0
V165	21 29 58.79	12 10 03.7	0.4339	0.6251	RR0
V166	21 29 59.38	12 10 01.1	0.3669	0.3656	RR1
V167	21 29 59.83	12 10 03.7	0.47	0.3192	RR1
V168	21 29 59.72	12 10 05.8	0.7225	0.6029	RR0

Table 1—Continued

Variable	RA h m s	Dec ° ' "	Previous period (d)	Our Period (d)	Type
V169	21 29 59.36	12 10 09.0	0.5555	0.5549	RR0
V170	21 29 58.81	12 09 21.9	0.6817	0.6781	RR0
V171	21 29 59.82	12 09 40.0	0.4578	0.5527	RR0
V172	21 29 59.94	12 09 49.1	0.5443	0.4317	RR01
V173	21 30 00.06	12 10 01.8	0.3747	0.3784	RR1
V174	21 30 00.20	12 10 13.5	0.2821	0.4006	RR01
V175	21 30 00.48	12 10 13.6	0.4282	0.7540	RR0
V177	21 29 57.67	12 10 14.9	0.407	0.4116	RR01
V178	21 29 58.02	12 10 19.3	0.286	0.4009	RR01
V181	21 29 59.81	12 10 25.1	0.5868	0.2232	RR01
ZK3	21 30 01.17	12 10 11.0	none	0.6310	RR0
ZK4	21 30 00.91	12 09 56.1	none	0.3829	RR1
ZK5	21 30 00.87	12 09 56.8	none	0.3647	RR1
ZK6	=V 175				RR0
ZK10	=V 174				RR1
ZK11	=V 173				RR1
ZK13	=V 172				RR1
ZK14	=V 181				RR0
ZK18	=V 162				RR0
ZK22	=V 166				RR1

Table 1—Continued

Variable	RA	Dec	Previous period	Our Period	Type
	h m s	° ' "	(d)	(d)	
ZK23	=V 169				RR0
ZK32	=V 165				RR0
ZK34	21 29 58.75	12 09 28.7	none	0.2977	RR1?
ZK39	=V 161				RR0
ZK44	=V 139				RR1
ZK52	=V 160				RR1
ZK55	=V 178				RR1
ZK63	21 29 57.81	12 10 21.0	none	0.4020	RR01
ZK64	=V 177				RR1
ZK67	21 29 57.45	12 09 43.6	none	0.5709	RR0
ZK69	21 29 57.13	12 10 21.4	none	0.4168	RR01
ZK74	21 29 56.25	12 10 30.9	none	0.3197	RR1
ZK78	21 29 55.90	12 10 27.8	none	0.4256	RR1
ZK80	21 29 55.86	12 10 09.2	none	0.3873	RR1
NV1	21 29 53.93	12 11 13.6	none	0.0585	SX Phe
NV2	21 29 56.22	12 09 37.9	none	0.4166	RR1?
NV3	21 29 58.50	12 10 40.2	none	0.4210	RR01?
NV4	21 29 58.89	12 09 02.7	none	0.3776	RR1
NV5	21 29 59.42	12 09 13.4	none	0.6101	RR0
NV6	21 30 02.69	12 10 31.9	none	0.3909	RR1

Table 1—Continued

Variable	RA h m s	Dec ° ' "	Previous period (d)	Our Period (d)	Type
NV7	21 30 00.40	12 09 57.8	none	0.3854	RR1
NV8	21 30 00.84	12 09 43.4	none	0.6294	RR0
NV9	21 30 02.93	12 10 09.5	none	0.3915	RR1
NV10	21 30 03.13	12 10 32.4	none	0.7594	RR0
NV11	21 29 59.55	12 09 23.6	none	0.2957	RR01
NV12	21 29 59.31	12 09 24.3	none	0.4104	RR01
NV13	21 30 00.03	12 09 39.3	none	0.3208	?
NV14	21 29 59.32	12 09 29.1	none	0.2993	RR1

Table 2. M15 Variables: Positions Relative to the Cluster Center

Variable	prev x (arcsec)	prev y (arcsec)	our x (arcsec)	our y (arcsec)	comment	difference (arcsec)
V11	172.30	−21.80	171.67	−21.43		0.73
V37	−25.20	−77.40	−25.69	−77.27		0.51
V39	20.50	−124.80	20.18	−124.45		0.47
V47	45.70	−4.30	43.49	−3.78		2.27
V53	−92.60	−111.00	−92.29	−110.50		0.59
V58	−55.60	8.80	−56.06	8.68		0.48
V60	53.40	−59.30	52.92	−59.21		0.49
V61	−67.30	−40.20	−67.47	−41.21		1.03
V63	49.80	31.00	48.11	30.76		1.71
V68	−31.80	12.60	−32.11	12.41		0.36
V69	−37.00	−25.20	−37.19	−25.63		0.47
V70	−34.00	−19.20	−34.38	−19.25		0.38
V71	−34.80	−12.60	−34.96	−12.45		0.22
V73	−3.70	20.00	−4.05	20.12		0.37
V75	2.20	−30.30	2.16	−30.99		0.69
V76	0.70	−28.90	0.70	−28.78		0.12
V77	−11.80	−22.90	−11.04	−22.51		0.85
V80	−47.40	−26.60	−47.61	−26.56		0.21
V81	−21.50	−5.90	−21.87	−5.04		0.94
V82	−20.10	2.40	−21.12	1.95		1.11
V83	16.30	−7.40	15.73	−6.40		1.15

Table 2—Continued

Variable	prev x (arcsec)	prev y (arcsec)	our x (arcsec)	our y (arcsec)	comment	difference (arcsec)
V84	17.53	−14.20	17.47	−14.30		0.12
V86	12.60	4.40	12.66	4.32		0.10
V88	2.20	26.60	1.69	26.48		0.52
V89	−23.70	−6.70	−23.78	−7.13		0.44
V90	31.10	4.40	31.76	4.49		0.67
V91	67.30	28.90	67.20	27.54		1.36
V92	9.60	−25.20	9.96	−25.34		0.39
V93	27.40	−33.30	29.03	−33.77		1.70
V94	3.70	28.90	2.43	28.27		1.42
V97	−79.50	29.30	−79.96	29.22		0.47
V106	−30.30	12.80	−32.11	13.91		2.12
V111	41.70	−0.70	42.32	−0.08		0.88
V114	0.91	49.93	−1.78	49.88		2.69
V117	15.84	−36.80	14.49	−35.87		1.64
V118	17.60	55.67	19.37	52.74		3.42
V119	20.74	3.51	19.57	4.37		1.45
V128	1.03	−0.86	−1.00	1.40		3.04
V129	−7.28	−14.02	−6.88	−14.00		0.40
V130	−6.95	−10.71	−6.11	−10.68		0.84
V131	−7.05	−2.23	−6.71	−2.21		0.34

Table 2—Continued

Variable	prev x (arcsec)	prev y (arcsec)	our x (arcsec)	our y (arcsec)	comment	difference (arcsec)
V134	−4.44	−3.79	−4.30	−3.79		0.14
V136	−2.24	4.20	−1.36	4.49		0.93
V137	−0.71	2.52	−0.58	2.54		0.13
V138	3.07	−4.12	3.58	−4.35		0.56
V139	1.43	8.38	0.98	7.54	ZK44	0.95
V141	9.23	0.41	9.03	0.49		0.22
V142	3.86	−2.11	4.37	−2.15		0.51
V144	13.89	−1.81	14.13	−1.76		0.25
V145	14.38	0.31	15.03	0.32		0.65
V155	−10.64	7.23	−10.58	7.25		0.06
V159	0.92	−0.23	0.46	−0.50		0.53
V160	−3.85	−14.43	−3.24	−14.46	ZK52	0.61
V161	2.89	−13.45	2.79	−13.6	ZK39	0.18
V162	18.39	−13.00	18.06	−13.21	ZK18	0.39
V163	13.63	−10.70	13.66	−10.88		0.18
V164	3.05	3.70	2.82	3.48	ZK37	0.32
V165	6.73	0.69	6.93	0.56	ZK32	0.24
V166	15.78	−2.01	15.59	−2.10	ZK22	0.21
V167	22.68	0.70	22.20	0.46		0.54
V168	20.99	2.74	20.59	2.57		0.43

Table 2—Continued

Variable	prev x (arcsec)	prev y (arcsec)	our x (arcsec)	our y (arcsec)	comment	difference (arcsec)
V169	15.47	5.97	15.31	5.80	ZK23	0.23
V170	7.04	−41.27	7.14	−41.21		0.12
V171	22.53	−23.08	22.01	−23.03		0.52
V172	24.21	−13.99	23.64	−15.24	ZK13	1.37
V173	26.21	−1.19	25.58	−1.47	ZK11	0.69
V174	28.20	10.52	27.66	10.21	ZK10	0.62
V175	32.65	10.62	31.77	10.28	ZK6	0.94
V177	−10.45	11.80	−9.50	11.86	ZK64	0.95
V178	−5.08	16.19	−4.35	16.22	ZK55	0.73
V181	22.37	22.11	21.95	21.84	ZK14	0.50
ZK3	41.65	7.61	41.90	7.62		0.25
ZK4	37.66	−7.09	38.05	−7.25		0.42
ZK5	37.26	−6.84	37.46	−6.54		0.36
ZK6	31.51	10.34	31.77	10.28	V175	0.27
ZK10	27.30	10.25	27.66	10.21	V174	0.36
ZK11	25.27	−1.47	25.58	−1.47	V173	0.31
ZK13	23.29	−14.21	23.64	−15.44	V172	1.28
ZK14	21.82	21.92	21.95	21.84	V181	0.15
ZK18	17.70	−13.16	18.06	−13.21	V162	0.36
ZK22	15.27	−2.06	15.59	−2.10	V166	0.32

Table 2—Continued

Variable	prev x (arcsec)	prev y (arcsec)	our x (arcsec)	our y (arcsec)	comment	difference (arcsec)
ZK23	15.07	5.78	15.31	5.80	V169	0.24
ZK32	6.65	0.70	6.93	0.56	V165	0.31
ZK34	5.85	−34.44	6.27	−34.41		0.42
ZK37	3.12	3.63	2.82	3.48	V164	0.34
ZK39	2.91	−13.46	2.79	−13.60	V161	0.18
ZK44	1.21	7.25	1.51	7.09	V139	0.34
ZK47	0.81	−1.94	0.31	−1.90		0.50
ZK52	−3.54	−14.54	−3.24	−14.46	V160	0.31
ZK55	−4.49	16.33	−4.35	16.22	V178	0.18
ZK62	−7.39	−8.70	−7.04	−8.64	Phe	0.36
ZK63	−7.68	18.19	−7.43	17.94		0.35
ZK64	−9.75	11.73	−9.50	11.86	V177	0.28
ZK67	−13.04	−19.32	−12.79	−19.40		0.26
ZK69	−17.58	18.47	−17.41	18.41		0.18
ZK74	−30.51	28.17	−30.32	27.99		0.26
ZK78	−35.53	25.13	−35.47	24.93		0.21
ZK80	−36.27	6.46	−36.09	6.34		0.22

Table 3. M15 Variables

Variable	$\langle V \rangle_{\text{mag}}$	$\langle V \rangle_{\text{int}}$	A_V	$\langle B \rangle_{\text{mag}}$	$\langle B \rangle_{\text{int}}$	A_B	$\langle I \rangle_{\text{mag}}$	$\langle I \rangle_{\text{int}}$	A_I
V1	15.009	14.954	0.99	15.412	15.317	1.26	14.385	14.362	0.69
V6	15.797	15.757	0.94	16.224	16.180	1.14	15.156	15.142	0.54
V7	15.770	15.754	0.56	16.180	16.157	0.65	15.316	15.306	0.32
V8	15.795	15.763	0.89	16.241	16.190	1.05	15.178	15.163	0.51
V9	15.711	15.685	0.84	16.110	16.068	1.05	15.137	15.126	0.79
V10	15.869	15.856	0.50	16.214	16.191	0.65	15.413	15.407	0.36
V13	15.978	15.944	1.01	16.384	16.323	1.18	15.386	15.372	0.65
V16	15.854	15.843	0.36	16.186	16.169	0.47	15.356	15.352	0.23
V17	15.753	15.743		16.104	16.086		15.274	15.270	
V18	15.846	15.829	0.55	16.185	16.157	0.70	15.397	15.391	0.34
V19	15.812	15.733	1.38	16.173	16.052	1.69	15.319	15.291	0.90
V20	15.779	15.751	0.90	16.266	16.220	1.09	15.137	15.129	0.42
V21	15.705	15.669	0.85	16.139	16.073	1.20	15.025	15.012	0.49
V24	15.877	15.859	0.50	16.216	16.188	0.78	15.341	15.336	0.37
V32	15.774	15.735	0.97	16.194	16.131	1.22	15.205	15.192	0.64
V33	15.776	15.732	1.05	16.180	16.105	1.31	15.196	15.178	0.68
V36	15.853	15.817	0.93	16.268	16.202	1.15	15.208	15.195	0.59
V37	15.885	15.871	0.53	16.180	16.157	0.69	15.474	15.467	0.33
V38	15.839	15.820	0.55	16.200	16.173	0.73	15.338	15.334	0.29
V39	15.892	15.880		16.274	16.258		15.397	15.390	
V40	15.885	15.867		16.213	16.185		15.346	15.336	

Table 3—Continued

Variable	$\langle V \rangle_{\text{mag}}$	$\langle V \rangle_{\text{int}}$	A_V	$\langle B \rangle_{\text{mag}}$	$\langle B \rangle_{\text{int}}$	A_B	$\langle I \rangle_{\text{mag}}$	$\langle I \rangle_{\text{int}}$	A_I
V41	15.715	15.703		16.090	16.074		15.141	15.135	
V44	15.800	15.773	0.81	16.253	16.206	1.00	15.252	15.242	0.58
V45	15.694	15.651	0.91	16.166	16.099	1.12	15.089	15.076	0.53
V46	15.645	15.619	0.74	16.141	16.102	0.90	15.028	15.019	0.46
V47	15.711	15.676	0.96	16.177	16.126	1.18	15.029	15.017	0.63
V48	15.887	15.870	0.63	16.193	16.162	0.70	15.418	15.411	0.38
V49	15.896	15.872	0.81	16.289	16.243	1.07	15.245	15.241	0.56
V50	15.945	15.927		16.171	16.134		15.563	15.553	
V51	15.827	15.816	0.45	16.192	16.176	0.58	15.334	15.329	0.33
V53	15.828	15.822		16.213	16.203		15.310	15.305	
V54	15.745	15.734	0.48	16.159	16.143	0.59	15.255	15.251	0.33
V55	15.746	15.732	0.67	16.277	16.254	0.75	15.076	15.071	0.39
V56	15.780	15.741	1.02	16.249	16.180	1.21	15.156	15.142	0.60
V57	15.793	15.773	0.58	16.142	16.113	0.69	15.350	15.343	0.36
V58	15.830	15.825		16.214	16.206		15.152	15.145	
V59	15.855	15.797	1.13	16.274	16.174	1.44	15.327	15.307	0.70
V60	15.612	15.598	0.61	16.159	16.137	0.73	14.927	15.921	0.46
V61	15.802	15.794		16.236	16.225		15.205	15.203	
V62	15.741	15.726	0.53	16.062	16.042	0.61	15.210	15.205	0.30
V63	15.776	15.753	0.71	16.307	16.259	0.94	15.105	15.095	0.42
V64	15.765	15.761	0.58	16.145	16.119	0.65	15.207	15.162	0.38

Table 3—Continued

Variable	$\langle V \rangle_{\text{mag}}$	$\langle V \rangle_{\text{int}}$	A_V	$\langle B \rangle_{\text{mag}}$	$\langle B \rangle_{\text{int}}$	A_B	$\langle I \rangle_{\text{mag}}$	$\langle I \rangle_{\text{int}}$	A_I
V65	15.802	15.791	0.54	16.317	16.294	0.56	15.145	15.140	0.34
V66	15.892	15.882		16.250	16.232		15.389	15.384	
V67	15.881	15.874		16.251	16.238		15.303	15.297	
V68	15.773	15.757	0.50	16.185	16.165	0.65	15.181	15.167	
V69	16.002	15.977	1.03	16.536	16.499	1.16	15.236	15.224	0.58
V70	15.854	15.844	0.49	16.279	16.265	0.53	15.217	15.209	0.38
V71	15.884	15.870	0.60	16.301	16.274	0.73	15.238	15.225	
V73	15.767	15.753		16.176	16.169	0.43	15.216	15.199	
V74	15.883	15.862	0.56	16.186	16.155	0.73	15.440	15.432	0.38
V75	15.872	15.855	0.50	16.306	16.284	0.72	15.259	15.253	
V76	15.871	15.864	0.40	16.316	16.303	0.50	15.217	15.207	
V77	15.697	15.681	0.71	16.118	16.075	0.98	15.051	15.027	
V78	15.699	15.676	0.89	16.246	16.215	1.04	15.103	15.095	0.70
V80	15.720	15.697	0.72	16.265	16.228	0.86	15.058	15.045	
V81	15.812	15.791		16.348	16.325		15.061	15.055	
V82	15.664	15.656		16.154	16.144	0.55	15.043	15.027	
V83	15.587	15.578	0.95	16.223	16.187	1.04	15.002	14.985	
V84	16.031	15.989	1.05	16.491	16.430	1.12	15.435	15.415	
V86	13.669	13.659		14.380	14.368		12.659	12.646	
V87	15.961	15.943	0.65	16.264	16.236	0.75			
V88	15.592	15.567	0.80	16.091	16.058	0.96	14.840	14.818	

Table 3—Continued

Variable	$\langle V \rangle_{\text{mag}}$	$\langle V \rangle_{\text{int}}$	A_V	$\langle B \rangle_{\text{mag}}$	$\langle B \rangle_{\text{int}}$	A_B	$\langle I \rangle_{\text{mag}}$	$\langle I \rangle_{\text{int}}$	A_I
V89	15.791	15.785		16.255	16.250		15.082	15.076	
V90	15.754	15.742	0.48	16.151	16.124	0.83	15.210	15.202	
V92	15.804	15.798		16.311	16.303	0.44	15.143	15.129	
V93	15.820	15.810	0.40	16.218	16.202	0.49	15.176	15.171	
V97	15.779	15.765	0.63	16.240	16.209	0.81	15.143	15.136	0.42
V111				16.663	16.663				
V117				17.020	17.019				
V118	15.847	15.836	0.49	16.133	16.118	0.58	15.389	15.384	
V119	16.050	16.046		16.728	16.727	0.35	15.099	15.091	
V130	15.443	15.347		16.097	16.047	0.95	14.707	14.613	
V131				15.677	15.653	0.80			
V139				15.920	15.906	0.55			
V141	15.546	15.533		15.985	15.978	0.56	14.915	14.887	
V160=ZK52	15.808	15.741		15.903	15.894	0.60	15.133	14.863	
V162=ZK18				16.159	16.140	0.85			
V163	15.722	15.674		16.043	16.004	1.19	14.970	14.945	
V166=ZK22	15.447	15.424	0.53	15.884	15.866	0.67	14.767	14.754	
V167	15.538	15.531		15.940	15.931	0.60	14.764	14.759	
V168	15.734	15.717		16.230	16.201	0.93	15.005	14.994	
V169=ZK23	15.840	15.807	1.00	16.409	16.345	1.35	15.074	15.033	
V170	15.735	15.713	0.63	16.248	16.225	0.77	15.141	15.112	

Table 3—Continued

Variable	$\langle V \rangle_{\text{mag}}$	$\langle V \rangle_{\text{int}}$	A_V	$\langle B \rangle_{\text{mag}}$	$\langle B \rangle_{\text{int}}$	A_B	$\langle I \rangle_{\text{mag}}$	$\langle I \rangle_{\text{int}}$	A_I
V171	15.818	15.801		16.294	16.261	0.84	15.131	15.121	
V172	15.113	15.112	0.20	15.964	15.958	0.35			
V173=ZK11	15.748	15.737	0.46	16.212	16.192	0.69	15.053	15.048	
V177=ZK64	15.585	15.578	0.32	16.075	16.066	0.54	14.900	14.891	
V178=ZK55	15.750	15.741	0.34	16.212	16.199	0.48	15.142	15.124	
V181=ZK14				16.015	16.013				
ZK4	15.812	15.801	0.45	16.222	16.209	0.53	15.161	15.151	
ZK5	15.767	15.751	0.55	16.181	18.173	0.63	15.284	15.273	
ZK34	15.819	15.760		16.218	16.202	0.70	15.015	14.929	
ZK63	15.594	15.587	0.35	16.014	16.005	0.50	15.007	15.003	
ZK67				16.463	16.340	1.40			
ZK69				16.090	16.085	0.40			
ZK74	15.805	15.787	0.53	16.135	16.109	0.88	15.293	15.284	
ZK78	15.737	15.727	0.36	16.120	16.117	0.54	15.159	15.156	0.23
ZK80	15.789	15.781	0.37	16.237	16.223	0.54	15.163	15.159	
NV1	17.950	17.933		18.338	18.325	0.60	17.412	17.400	
NV2				16.236	16.229				
NV3	15.671	15.658	0.40	16.083	16.072	0.55	15.151	15.137	
NV5	15.760	15.725	0.85	16.241	16.225	1.13	15.107	15.012	
NV6	15.779	15.773	0.32	16.192	16.181	0.42	15.220	15.217	0.25
NV7	15.740	15.731	0.38	16.142	16.125	0.52	15.148	15.143	0.26

Table 3—Continued

Variable	$\langle V \rangle_{\text{mag}}$	$\langle V \rangle_{\text{int}}$	A_V	$\langle B \rangle_{\text{mag}}$	$\langle B \rangle_{\text{int}}$	A_B	$\langle I \rangle_{\text{mag}}$	$\langle I \rangle_{\text{int}}$	A_I
NV9	15.826	15.813	0.45	16.370	16.349	0.56	15.158	15.147	
NV10	15.792	15.782	0.35	16.292	16.281	0.45	15.151	15.147	0.24
NV11				16.266	16.257				
NV12				16.169	16.155				
NV13				16.077	16.075	0.56			
NV14	15.812	15.807	0.31	16.090	16.081	0.43	15.339	15.333	